Eur. Phys. J. Plus (2016) **131**: 380
DOI 10.1140/epjp/i2016-16380-3

THE EUROPEAN PHYSICAL JOURNAL PLUS

Regular Article

Quantum correlations dynamics and decoherence of a three-qubit system subject to classical environmental noise

Martin Tchoffo[1,a], Lionel Tenemeza Kenfack[1], Georges Collince Fouokeng[1,2], and Lukong Cornelius Fai[1]

[1] Mesoscopic and Multilayer Structure Laboratory, Department of Physics, Faculty of Science, University of Dschang, PO Box: 67 Dschang, Cameroon
[2] Laboratoire de Génie des Matériaux, Pôle Recherche-Innovation-Entrepreneuriat (PRIE), Institut Universitaire de la Côte, BP 3001 Douala, Cameroon

Received: 22 July 2016 / Revised: 4 October 2016
Published online: 31 October 2016 –

Abstract. We address the dynamics of decoherence and quantum correlations (entanglement and discord) in a model of three non-interacting qubits, initially prepared in a maximally entangled pure Greenberger-Horne-Zeilinger (GHZ) state and then subjected to classical environmental noise in common, different and mixed environments. The noise is modeled by randomizing the single-qubit transition amplitudes. We address both static and colored environmental noise. We find that the dynamics of quantum correlations are strongly affected by the type of system-environment interaction and the kind of the noise considered. On the one hand, our results clearly show that unlike what was found in the case of the two-qubit model analogous to the one here investigated, quantum correlations are not totally destroyed when the qubits are coupled to the noise in a common environment. On the other hand, the presence or absence of peculiar phenomena, such as entanglement, revivals and sudden death are observed. Furthermore, we show that the partial preservation of entanglement can be successfully detected by means of the suitable entanglement witness. Finally, in the case of static noise we find that the decoherence becomes stronger as the disorder of the environment increases whereas, for colored noise, it becomes stronger as the number of fluctuators increases.

1 Introduction

In recent years, quantum correlations have become the main focus of fundamental research in the discipline of quantum information theory [1]. At the very beginning of the foundation of quantum information science, how to classify and quantify the quantum correlations encoded in a given state has attracted significant attention as one of the most fundamental and central research topics. Entanglement is an important aspect of quantum systems which demonstrates correlations that cannot be discussed classically [2]. This quantity plays a central role in many fields of research, such as quantum computation [3], quantum information processing [4,5], cryptography [6], quantum dense coding [7], sensitive measurements [8], quantum telecloning [9] and entanglement swapping [10], just to cite a few examples. However, the major limitation of the use of entangled systems in practical applications is due to the unavoidable interaction of the real quantum systems with their surroundings, resulting in the loss of their correlations and, consequently, of their efficiency to perform quantum communication tasks [11–14]. Hence, noise represents one of the unavoidable physical phenomena in the context of quantum information and computations [15] and it is therefore of great significance to examine the effect of the various kinds of environmental noise on the dynamics of quantum correlations in realistic quantum systems and to search for possible approaches to protect the quantum correlations from the influence of its environments. Recently, the effect of different kinds of classical environmental noise on the dynamics of quantum correlations for two non-interacting qubits has been investigated both theoretically [16–21] and experimentally [22,23]. Its extension to a tripartite system within the random telegraph noise (RTN) is proposed by Fabrizio Buscemi and Paolo Bordone [24]. Practically speaking, while the quantification of bipartite quantum entanglement is well known [25–27], no matter whether the state is pure or mixed, its extensions to the multipartite case is still much more complicated and the difficulty grows up exponentially, even for the simplest tripartite case [28]. Therefore, only recently the time

[a] e-mail: mtchoffo2000@yahoo.fr

evolution of the entanglement has begun to be analyzed in multipartite open quantum systems. In literature, different approaches, such as tripartite negativity [29] and concurrence [30], have been proposed to characterize the tripartite and multipartite entanglement. However, many of these proposals are only eligible for pure states and none of them could give a perfectly defined quantification. In addition, it is worth noting that tripartite negativity cannot distinguish the entanglement of a genuine tripartite entangled state from that of a bi-separable state in a generalized sense.

A different tool for understanding entanglement of three and more qubits is the use of so-called entanglement witness (EW), namely suitable observable that, at least in principle, can be experimentally implemented to detect the presence of entanglement [31,32]. However, recent developments in the field of quantum information processing showed that the entanglement is not the only kind of quantum correlations useful for quantum information processing [33–35]. It has shown both theoretically [36] and experimentally [37] that some tasks can be speed up over their classical counterparts using fully separable and highly mixed states [38]. Thus, in order to take into account these correlations, many quantifiers were proposed in recent years [39], among which the most used is certainly quantum discord (QD) [38] which can be expressed in terms of the difference between the total and the classical correlations for a system when one of its sub-parties is subject to an unobserved measure process. Recently, QD has been intensively investigated in the literature and its definition has been generalized to multipartite systems according to different approaches. Note that such a quantity, however, significantly depends upon both the subsystem chosen and the measurement performed on it; in particular, if the measurement is carefully selected, we can minimize its *disturbing effect* on the system [40]. There are, in general, two kinds of quantum discord: measurement-based discord and distance-based discord [38]. Under suitable conditions, quantum discord has been proved to be more robust against decoherence than entanglement in noisy environments [41–46].

The aim of this paper is to analyze the role played by a classical noisy environment in to the dynamics of the quantum correlations and decoherence in a physical model consisting of three non-interacting qubits. The influence of the classical environmental noise on the system is described by means of a stochastic Hamiltonian with a coupling term mimicking a static signal or the $1/f^{\alpha}$ spectrum. It is worth noting that a noise with spectrum of the form $1/f^{\alpha}$ is among the main sources of decoherence in quantum solid-state devices, superconducting qubits, and magnetic systems [47–49]. The exponent α appearing in the spectrum is a positive number. The cases with $\alpha = 1$ and $\alpha = 2$ are often called pink and brown noise, respectively. Environments characterized by $1/f^{\alpha}$ noise spectra usually arise when a system is coupled to a large number of bistable fluctuators, with a specific distribution of their switching rates. Upon considering a collection of fluctuators, the colored noise may be implemented by means of a linear combination of sources of RTN, each characterized by a specific switching rate chosen from a suitable distribution [50].

The dynamics of the three qubits is evaluated by averaging the time-evolved states over the noise phase. In order to fully characterize quantum correlations, we employ suitable measures for tripartite quantum discord, entanglement and decoherence. In this work the entanglement is quantified in terms of tripartite negativity, which was shown to play a key role in quantum information protocols since states exhibiting nonzero tripartite negativity are distillable to GHZ states [24]. The other estimator is the use of the concept of entanglement witness. We employ the Von Neumann entropy as a measure for decoherence. Note that, unlike tripartite negativity, in order to quantify the three qubits QD we need to use numerical techniques apt to optimize, over positive-operator–valued measures (POVMs) and subsystems, the conditional entropies appearing in the definition of discord. In this work, QD is numerically quantified by using the approach developed in ref. [51].

The paper is organized as follows: In sect. 2 we introduce the genuine quantifiers for correlations and decoherence in tripartite quantum systems. In sect. 3, we illustrate the physical model consisting of three non-interacting qubits subject to a classical noisy environment within common, different and mixed environments. In sect. 4 we report the time evolution of quantum correlations and decoherence for both static and colored noise in the case of common, different and mixed system-environments coupling. Finally, in sect. 5 some conclusions are drawn.

2 Quantum correlation measures in tripartite systems

Here, we illustrate the correlation measures adopted in this work to quantify entanglement, decoherence, and tripartite quantum discord.

2.1 Measures for entanglement

2.1.1 Tripartite negativity

As we have pointed out in the introduction, there are several kinds of definitions of entanglement measure of the three-qubit system. In this paper, we explore a valid measure of tripartite entanglement for mixed state $\rho \equiv \rho_{abc}$ by

means of the tripartite negativity [52], which is the geometric mean of the bipartite negativities of any bipartition of the system given by

$$\mathcal{N}^{(3)}(\rho_{abc}) = \sqrt[3]{\mathcal{N}_{a|bc} + \mathcal{N}_{b|ac} + \mathcal{N}_{c|ab}}, \tag{1}$$

where $\mathcal{N}_{I|JK} = \sum_i |\lambda_i(\rho^{T_I})| - 1$ is the bipartite negativity between the subsystem I and the compound system JK with $I \in \{a, b, c\}$ and $JK \in \{ab, ac, bc\}$. $\lambda_i(\rho^{T_I})$ denote the i-th eigenvalues of the density matrix ρ after taking partial transpose with respect to subsystem I. Recently, tripartite negativity has also been used to estimate the entanglement of tripartite system within the random telegraph noise [24]. For symmetrical tripartite quantum systems as in our case of study, $\mathcal{N}_{a|bc} = \mathcal{N}_{b|ac} = \mathcal{N}_{c|ab}$ and consequently $\mathcal{N}^{(3)}(\rho)$ reduce to the bipartite negativity.

2.1.2 Entanglement witnesses

A different tool for understanding entanglement of three and more qubits is the use of so-called *entanglement witness* [53], namely suitable observable that, at least in principle, can be experimentally implemented to detect the presence of entanglement [31, 32]. An entanglement witness is an operator ($\mathcal{W}$) which has the property that $\mathrm{Tr}(\rho\mathcal{W}) < 0$ indicate the appearance of tripartite entanglement experimentally detectable in the system. However, $\mathrm{Tr}(\rho\mathcal{W}) > 0$ do not guarantee the absence of entanglement. Note that, $\mathrm{Tr}(\rho\mathcal{W}) < 0$ is a sufficient but not a necessary condition for identifies the state ρ as an entangled state. It is worth noting that any given entanglement witness operator will identify some but not all entangled states, and in general many different entanglement witness operators exist. For the three-qubit GHZ-type states the relevant witnesses are [54]

$$\mathcal{W}_{GHZ1} = \frac{1}{2}\mathbb{I} - \left|GHZ\right\rangle\left\langle GHZ\right| \tag{2}$$

and

$$\mathcal{W}_{GHZ2} = \frac{3}{4}\mathbb{I} - \left|GHZ\right\rangle\left\langle GHZ\right|. \tag{3}$$

Specifically, in this work we will use the witness operator $\mathcal{W}_{GHZ1}$ that permit to identify whether a state is in the W-B class, namely a state with true tripartite entanglement either of the GHZ-type or W-type and not bi-separable [24].

2.2 Measure for decoherence

In quantum information processing, decoherence is another essential problem that deserves some attention. Generally, decoherence is used to estimate the deviation from an ideal state [55]. To some extent, decoherence is an evaluator of the degree of entanglement between the system and the noisy environment. In this paper, decoherence is estimated by means of the Von Neumann entropy [56] of the time-evolved density matrix of the system:

$$\varepsilon_\vartheta(t) = -\,\mathrm{Tr}\left[\rho(t)\ln\rho(t)\right]. \tag{4}$$

2.3 Measure for quantum discord

According to ref. [57] a state of n particles is said to possess genuine n-partite correlations when it is non-product in every bipartite cut. From this point of view, we can define the genuine tripartite total correlations $\mathcal{T}^{(3)}(\rho)$, of a mixed state ρ_{abc} as [51]

$$\mathcal{T}^{(3)}(\rho) = \mathcal{T}(\rho) - \mathcal{T}^{(2)}(\rho), \tag{5}$$

where $\mathcal{T}(\rho)$ is the quantum extension of the Shannon classical mutual information,

$$\mathcal{T}(\rho) = S(\rho_a) + S(\rho_b) + S(\rho_c) - S(\rho), \tag{6}$$

and $\mathcal{T}^{(2)}(\rho)$ is given by the maximum of the total bipartite correlations among two qubits of the system, namely

$$\mathcal{T}^{(2)}(\rho) = \max\left[I^{(2)}(\rho_{a,b}), I^{(2)}(\rho_{a,c}), I^{(2)}(\rho_{b,c})\right], \tag{7}$$

In the previous equations, $S(\rho_I)$ is the Von Neumann entropy of the corresponding reduced density matrix. $I^{(2)}(\rho_{I,J}) = S(\rho_I) + S(\rho_J) - S(\rho_{IJ})$, $I, J \in \{a, b, c\}$ denoting the bipartite quantum mutual information of the subsystem consisting of the two qubits I and J. From eqs. (5), (6) and (7) we obtain

$$\mathcal{T}^{(3)}(\rho) = \min\left[I^{(2)}(\rho_{a,bc}), I^{(2)}(\rho_{b,ac}), I^{(2)}(\rho_{c,ab})\right], \tag{8}$$

where $I^{(2)}(\rho_{I,JK})$ is the mutual information between one-qubit part and the left two-qubit part.

We can also define the genuine tripartite classical correlations $\mathcal{J}^{(3)}(\rho)$ as

$$\mathcal{J}^{(3)}(\rho) = \mathcal{J}(\rho) - \mathcal{J}^{(2)}(\rho), \tag{9}$$

where

$$\mathcal{J}(\rho) = \max_{I,J,K} \left[S(\rho_I) + S(\rho_K) - S(\rho_{I|J}) - S(\rho_{K|IJ})\right] \tag{10}$$

and

$$\mathcal{J}^{(2)}(\rho) = \max\left[J^{(2)}(\rho_{a,b}), J^{(2)}(\rho_{a,c}), J^{(2)}(\rho_{b,c})\right]. \tag{11}$$

In agreement with ref. [58] the tripartite quantum discord $\mathcal{D}^{(3)}$ can be expressed as the difference between the genuine tripartite total correlations and the genuine tripartite classical correlations,

$$\mathcal{D}^{(3)}(\rho) = \mathcal{T}^{(3)}(\rho) - \mathcal{J}^{(3)}(\rho). \tag{12}$$

For symmetrical tripartite systems, *i.e.* systems whose state is invariant under the permutations of the three parties, it can be shown that the genuine tripartite total and classical correlations can be regarded as

$$\mathcal{T}^{(3)}(\rho) = S(\rho_c) + S(\rho_{ab}) - S(\rho) \tag{13}$$

and

$$\mathcal{J}^{(3)}(\rho) = S(\rho_c) - S(\rho_{c|ab}). \tag{14}$$

We can then easily compute that

$$\mathcal{D}^{(3)}(\rho) = S(\rho_{ab}) + S(\rho_{c|ab}) - S(\rho), \tag{15}$$

where $S(\rho_{ab})$ is the Von Neumann entropy of the reduce density matrix ρ_{ab}, $S(\rho_{c|ab}) = \min_{\{E^{ab}_{ij}\}} \sum_{ij} P_{ij} S(\rho_{c|E^{ab}_{ij}})$ is the relative entropy of the qubit "c", when the projective measurement is carried out on the subsystem "ab". $\rho_{c|E^{ab}_{ij}} = \frac{\mathrm{Tr}_{ab}[(\mathbb{I}^c \otimes E^{ab}_{ij})\rho]}{P_{ij}}$ is the density matrix of the system after the measurement has been performed on the subsystem "ab". and $P_{ij} = \mathrm{Tr}[(\mathbb{I}^c \otimes E^{ab}_{ij})\rho]$ is the probability of obtaining the (i,j) outcomes. In the previous expressions, the operators $\{E^{ab}_{ij}\}$ are positive-operator–valued measures (POVMs) that act on the subsystem "ab" and whose outcomes are labeled with two indices (i,j). For sake of simplicity, we will replace the global POVM $\{E^{ab}_{ij}\}$ with the external product of two local POVMs $E^a_i \otimes E^b_j$, acting separately on parties "a" and "b". In our numerical approach the relative entropy $S(\rho_{c|ab})$ has been estimated by using orthogonal-projection–valued measures (PVMs), since they are easier to implement in the numerical minimization process. Hence, following Andrea Beggi *et al.* [59] we can define the external product of two local POVMs acting separately on parties "a" and "b" as

$$E^a_i \otimes E^b_j = |a_i\rangle\langle a_i| \otimes |b_i\rangle\langle b_i|, \tag{16}$$

with

$$\begin{cases} |a_1\rangle = \cos\theta_1|0\rangle + \exp(i\phi_1)\sin\theta_1|1\rangle, & |a_2\rangle = \sin\theta_1|0\rangle - \exp(i\phi_1)\cos\theta_1|1\rangle \\ |b_1\rangle = \cos\theta_2|0\rangle + \exp(i\phi_2)\sin\theta_2|1\rangle, & |b_2\rangle = \sin\theta_2|0\rangle - \exp(i\phi_2)\cos\theta_2|1\rangle \end{cases}, \tag{17}$$

where the angles θ_i and ϕ_i belong to the interval $[0, 2\pi]$.

3 The physical model

In this section, we describe a model consisting of three non-interacting qubits subject to noisy classical environment. The system-environment coupling is here analyzed in three different configurations as depicted in fig. 1. In the first configuration, each qubit is coupled to its own local environment. In the second configuration, two of the qubits are coupled in one common environment and the last one with its own local environment. In the third configuration all the qubits are coupled with the same environment.

In each of these configurations, the dynamics of the system is ruled by the stochastic Hamiltonian [24]

$$\mathcal{H}(t) = \mathcal{H}_a(t) \otimes \mathbb{I}_{bc} + \mathcal{H}_b(t) \otimes \mathbb{I}_{ac} + \mathcal{H}_c(t) \otimes \mathbb{I}_{ab}, \tag{18}$$

where $\mathbb{I}_{JK}$ is the identity operator acting in the subspace of the two qubits I and J, and $H_L(t)$ denotes the single-qubit Hamiltonian [16],

$$\mathcal{H}_L(t) = \varepsilon_L \mathbb{I}_L + \lambda \Delta_L(t) \sigma^x_L. \tag{19}$$

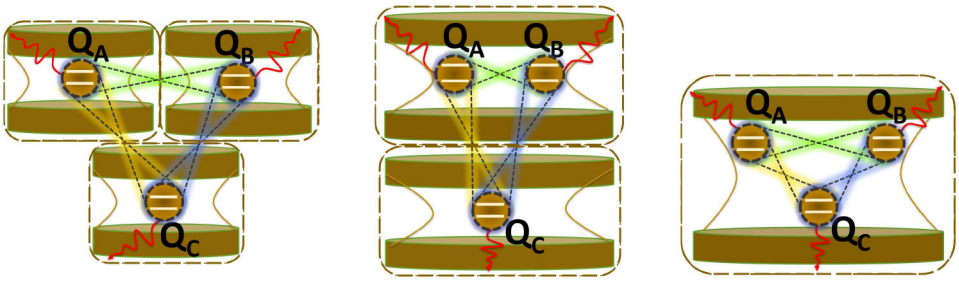

Fig. 1. Schematic of the system of three-qubit in different (left), mixed (center) and common (right) environments. The blue, yellow and green dotted lines represent the entanglement among the qubits, while the red wavy lines show the interaction of each subsystem with the classical environment.

$\mathbb{I}_L$ and σ_L^x indicating the identity operator and the Pauli matrix of the subspace of the qubit L. ε_L is the single-qubit energy in the absence of noise (energy degeneracy is assumed), λ is the system-environment coupling constant and $\Delta_L(t)$ is a random parameter which is use to introduce the classical noise. Note that, this model has already been used to evaluate the time behavior of entanglement and quantum discord for a system of three qubits subject to random telegraph noise [24].

Upon assuming $t_0 = 0$, the evolution operator for a given realization of the process Δ_L is expressed as

$$U_L(\Delta_L, t) = \exp\left[-i \int_0^t \mathcal{H}(s)\, \mathrm{d}s\right], \tag{20}$$

with $L \in \{a, b, c\}$. Since the three qubits are non-interacting, the corresponding evolution operator is given by

$$\begin{aligned} U(\varphi_a, \varphi_b, \varphi_c, t) = &\exp\left\{-i\left[\varepsilon_a t \mathbb{I}_a + \lambda \varphi_a(t)\sigma_a^x\right]\right\} \otimes \exp\left\{-i\left[\varepsilon_b t \mathbb{I}_b + \lambda \varphi_b(t)\sigma_b^x\right]\right\} \\ &\otimes \exp\left\{-i\left[\varepsilon_c t \mathbb{I}_c + \lambda \varphi_c(t)\sigma_c^x\right]\right\}, \end{aligned} \tag{21}$$

where we have introduced the noise phases $\varphi_L(t) = \lambda \int_0^t \Delta_L(s)\, \mathrm{d}s$. When the latter is applied to the initial state the specific system dynamics is obtained

$$\rho(\{\varphi\}, t) = U(\{\varphi\}, t)\rho(0)U(\{\varphi\}, t)^\dagger, \tag{22}$$

with $\{\varphi\} = \{\varphi_a, \varphi_b, \varphi_c\}$. Finally, the time-evolved density matrix describing the three qubits is evaluated by performing an average over the different noise configurations. As initial state, we consider a system prepared in pure GHZ state $\rho_0 = |\psi_{abc}\rangle\langle\psi_{abc}|$, with $|\psi_{abc}\rangle = \frac{1}{\sqrt{2}}(|0_a 0_b 0_c\rangle + |1_a 1_b 1_c\rangle)$. In appendices A and B the explicit evaluations of the time-evolved states for the various cases considered are reported: static and colored noise; different, common, and mixed environments.

3.1 Static noise

The static noise has already been used to study the dynamics of quantum correlations of two non-interacting qubits [16]. In agreement with this work, to model the static noise the adimensional parameters $\Delta_L(t)$ are assumed to be time-independent random variables following the flat probability distribution given by

$$P(\Delta_L) = \begin{cases} \dfrac{1}{\Delta_m} \longrightarrow |\Delta_L - \Delta_0| \leq \dfrac{\Delta_m}{2} \\ 0 \longrightarrow \text{otherwise} \end{cases}, \tag{23}$$

where Δ_0 denotes the mean value of the distribution and Δ_m quantifies the disorder of the environment; in fact, when Δ_m goes to zero, the noise effect vanishes. The autocorrelation function of Δ is given by $\langle \delta\Delta(t)\delta\Delta(0)\rangle = \Delta_m^2/12$. The static disorder represents an environment, whose memory effect cannot be neglected at any finite time, and therefore, the characteristic time of its correlations is always larger than the one of the environment-system coupling. Thus, this kind of noise is classify as non-Markovian noise [60]. On the other hand, for the case of local coupling to different environments, the time-evolved density matrix of the system at time t can be expressed as

$$\rho_{\mathrm{de}}(t) = \int_\alpha^\beta \int_\alpha^\beta \int_\alpha^\beta \rho_{\mathrm{de}}(\{\Delta\}, t)\, P(\Delta_a)\, P(\Delta_b)\, P(\Delta_c)\, \mathrm{d}\Delta_a\, \mathrm{d}\Delta_b\, \mathrm{d}\Delta_c, \tag{24}$$

where $\rho_{\rm de}(\{\Delta\},t) = U(\{\Delta\},t)\rho_0 U(\{\Delta\},t)^\dagger$ with $\{\Delta\} = \Delta_a, \Delta_b, \Delta_c$. For the case of qubits interacting in mixed environments, we assume that $\Delta_a = \Delta_b$ and thus the time-evolved density matrix of the system at time t reads

$$\rho_{\rm mix}(t) = \int_\alpha^\beta \int_\alpha^\beta \rho_{\rm mix}(\Delta_a, \Delta_c, t)\, P(\Delta_a)\, P(\Delta_c)\, {\rm d}\Delta_a\, {\rm d}\Delta_c, \tag{25}$$

where $\rho_{\rm mix}(\Delta_a, \Delta_c, t) = U(\Delta_a, \Delta_a, \Delta_c, t)\rho_0 U(\Delta_a, \Delta_a, \Delta_c, t)^\dagger$. Finally, when the qubits are coupled to a common environment, we assume that $\Delta_a = \Delta_b = \Delta_c$ and thus the time-evolved density matrix of the system at time t is given by

$$\rho_{\rm ce}(t) = \int_\alpha^\beta \rho_{\rm ce}(\Delta_a, t)\, P(\Delta_a)\, {\rm d}\Delta_a, \tag{26}$$

where $\rho_{\rm ce}(\Delta_a, t) = U(\Delta_a, \Delta_a, \Delta_a, t)\rho_0 U(\Delta_a, \Delta_a, \Delta_a, t)^\dagger$. In these expressions, we have: $\alpha = \Delta_0 - \frac{\Delta_m}{2}$ and $\beta = \Delta_0 + \frac{\Delta_m}{2}$.

3.2 Colored noise

The other kind of noise we examine is the $1/f^\alpha$ noise, which is ubiquitous in solid state devices. In agreement with ref. [47], in order to reproduce the $1/f^\alpha$ spectrum, the single RTN frequency power density must be integrated over the switching rates γ with a proper distribution,

$$S_{1/f^\alpha}(\omega) = \int_{\gamma_1}^{\gamma_2} S_{\rm RTN}(\omega, \gamma)\, P_\alpha(\gamma)\, {\rm d}\gamma, \tag{27}$$

where $S_{\rm RTN}(\omega,\gamma) = \frac{4\gamma}{(2\gamma)^2+\omega^2}$ is the random telegraph noise spectrum and we have explicitly wrote its dependency on the switching rate γ, $P_\alpha(\gamma)$ is the switching rate distribution and takes a different form depending on the kind of noise,

$$P_\alpha(\gamma) = \begin{cases} \dfrac{1}{\gamma \ln(\gamma_2/\gamma_1)} \longrightarrow \alpha = 1 \\ \dfrac{(\alpha-1)}{\gamma^\alpha}\left[\dfrac{(\gamma_1\gamma_2)^{\alpha-1}}{\gamma_2^{\alpha-1} - \gamma_1^{\alpha-1}}\right] \longrightarrow 1 < \alpha \leq 2 \end{cases}. \tag{28}$$

3.2.1 $1/f^\alpha$ noise from a single fluctuator

Here, the random parameters $\Delta_L(t)$ can only flip between two values ± 1 with a switching rate γ chosen from a distribution $P_\alpha(\gamma)$. The difference with the RTN case is that here the switching rate is not known *a priori*, but the fluctuator is described by a statistical mixture whose elements are taken from the ensemble $\{\gamma, P_\alpha(\gamma)\}$ with $\gamma \in [\gamma_1, \gamma_2]$. The qubits are affected only by one source of noise, and therefore only one decoherence channel is present. In order to describe the time-evolved density matrix of the three-qubit system, two ensemble averages are required.

The first average is over all the possible realizations of the noise phase:

$$\rho_{\rm de}(\gamma_a, \gamma_b, \gamma_c, t) = \left\langle \left\langle \left\langle U(\varphi_a, \varphi_b, \varphi_c, t)\rho(0)U(\varphi_a, \varphi_b, \varphi_c, t)^\dagger \right\rangle_{\varphi_a} \right\rangle_{\varphi_b} \right\rangle_{\varphi_c}, \tag{29}$$

$$\rho_{\rm mix}(\gamma_a, \gamma_c, t) = \left\langle \left\langle U(\varphi_a, \varphi_a, \varphi_c, t)\rho(0)U(\varphi_a, \varphi_a, \varphi_c, t)^\dagger \right\rangle_{\varphi_a} \right\rangle_{\varphi_c}, \tag{30}$$

and

$$\rho_{\rm ce}(\gamma_a, t) = \left\langle U(\varphi_a, \varphi_a, \varphi_a, t)\rho(0)U(\varphi_a, \varphi_a, \varphi_a, t)^\dagger \right\rangle_{\varphi_a}, \tag{31}$$

where $\rho(0)$ is the initial state of the three qubits, $\langle\cdots\rangle_{\varphi_L}$ denote the average over the possible values of the noise parameters and corresponds to the integral $\langle\cdots\rangle_{\varphi_L} = \int(\cdots)P(\varphi_L,t)\,{\rm d}\varphi_L$, where $P(\varphi_L,t)$ is the phase distribution and has the form [61,62]

$$\begin{aligned} P(\varphi_L,t) = \frac{1}{2}\,{\rm e}^{-\gamma_L t}\left\{[\delta(\varphi_L - \lambda t) + \delta(\varphi_L + \lambda t)] + \frac{\gamma_L}{\lambda}\left[\Theta(\varphi_L + \lambda t) + \Theta(\varphi_L - \lambda t)\right]\right\} \\ \times \left[\frac{I_1\left(\gamma_L t\sqrt{1-(\varphi_L/\lambda t)^2}\right)}{\sqrt{1-(\varphi_L/\lambda t)^2}} + I_0\left(\gamma_L t\sqrt{1-(\varphi_L/\lambda t)^2}\right)\right], \end{aligned} \tag{32}$$

where $\delta(x)$ is the Dirac delta function, $I_k(x)$ is the modified Bessel function and $\Theta(x)$ is the Heaviside step function.

The second average is over the possible choices for the switching rates γ in a range $[\gamma_1, \gamma_2]$

$$\rho_{\rm de}(t) = \int_{\gamma_1}^{\gamma_2}\int_{\gamma_1}^{\gamma_2}\int_{\gamma_1}^{\gamma_2} \rho_{\rm de}(\gamma_a,\gamma_b,\gamma_c,t)\, P_\alpha(\gamma_a)\, P_\alpha(\gamma_c)\, P_\alpha(\gamma_c)\, {\rm d}\gamma_a\, {\rm d}\gamma_b\, {\rm d}\gamma_c \tag{33}$$

$$\rho_{\rm mix}(t) = \int_{\gamma_1}^{\gamma_2}\int_{\gamma_1}^{\gamma_2} \rho_{\rm mix}(\gamma_a,\gamma_c,t) P_\alpha(\gamma_a) P_\alpha(\gamma_c)\, {\rm d}\gamma_a\, {\rm d}\gamma_c \tag{34}$$

and

$$\rho_{\rm ce}(t) = \int_{\gamma_1}^{\gamma_2} \rho_{\rm ce}(\gamma_a,t) P_\alpha(\gamma_a)\, {\rm d}\gamma_a. \tag{35}$$

Once the average over γ is performed, the time-evolved density matrix, $\rho_{\rm de}(t)$, $\rho_{\rm mix}(t)$ and $\rho_{\rm ce}(t)$ can be expressed in terms of time-dependent coefficients $H_{\rm de}(t)$ and $H_{\rm ce}(t)$. With

$$H_{\rm de}(t) = \left[\int_{\gamma_1}^{\gamma_2} \Phi_{2\lambda}(\gamma,t) P_\alpha(\gamma)\, {\rm d}\gamma\right]^2, \qquad H_{\rm ce}(t) = \int_{\gamma_1}^{\gamma_2} \Phi_{4\lambda}(\gamma,t) P_\alpha(\gamma)\, {\rm d}\gamma, \tag{36}$$

where the function $\Phi_{n\lambda}(\gamma,t)$ corresponds to the average phase factor $\langle \exp(in\lambda\varphi)\rangle$ and can be expressed as [62,63]

$$\Phi_{n\lambda}(\gamma,t) = \begin{cases} {\rm e}^{-\gamma t}\left[\cosh(\delta_{n\lambda}t) + \dfrac{\gamma}{\delta_{n\lambda}}\sinh(\delta_{n\lambda}t)\right] \to \gamma > n\lambda \\ {\rm e}^{-\gamma t}\left[\cos(\delta_{n\lambda}t) + \dfrac{\gamma}{\delta_{n\lambda}}\sin(\delta_{n\lambda}t)\right] \to \gamma < n\lambda \end{cases}, \tag{37}$$

with $\delta_{n\lambda} = \sqrt{|\gamma^2 - (n\lambda)^2|}, n \in \{1,2\}$.

3.2.2 $1/f^\alpha$ noise from a collection of fluctuators

We already stated that $1/f^\alpha$ noise may be obtained from a collection of N bistable fluctuators, each characterized by a switching rate γ_j and a Lorentzian power spectrum. In this case the random parameter in eq. (19) describes a linear combination of bistable fluctuators $\Delta_L(t) = \sum_{j=1}^N \Delta_{L,j}(t)$ where N is the number of fluctuator. Each $\Delta_{L,j}(t)$ has a Lorentzian power spectrum, whose sum gives the power spectrum of the noise [17]

$$S_{1/f^\alpha} = \sum_{j=1}^N S_j(\omega,\gamma_j) = \sum_{j=1}^N \frac{4\gamma_j}{(2\gamma_j)^2 + \omega^2}\,. \tag{38}$$

Here, we assume that all the fluctuators have the same coupling constant with the environment, that is $\lambda_j \equiv \lambda$. The global phase describes a linear combination of bistable fluctuators,

$$\varphi_L = \sum_{j=1}^N \varphi_{L,j}, \tag{39}$$

with $\varphi_{L,j} = -\lambda\int_0^t \Delta_{L,j}(s)\, {\rm d}s$. The global evolution operator $U_T(\{\varphi\},t)$ for fixed values of the parameters associated to each fluctuator reads

$$U_T(\{\varphi\},t) = U_a(\varphi_a,t)\otimes U_b(\varphi_b,t)\otimes U_c(\varphi_c,t), \tag{40}$$

with $U_L(\varphi_L,t) = \exp[-i(\varepsilon_L t\mathbb{I}_L - \varphi_L(t)\sigma_L^x)]$. Once more, the dynamics of the system density matrix can be written as

$$\rho(\{\gamma_j\},t) = \left\langle U_T(\{\varphi\},t)\rho(0)U_T(\{\varphi\},t)^\dagger\right\rangle_{\{\varphi\}}. \tag{41}$$

The evaluation of the global system density matrix $\rho(\{\gamma_j\},t)$ requires an estimate of the averaged terms of the type $\langle\cos(n\varphi_L(t))\rangle_{\varphi_L}$ and $\langle\sin(n\varphi_L(t))\rangle_{\varphi_L}$, which can be computed in terms of the coefficient $\Phi_{n\lambda}$ as follows:

$$\begin{cases} \langle\cos(n\varphi_L(t))\rangle_{\varphi_L} = \displaystyle\prod_{j=1}^N \Phi_{n\lambda}(\gamma_{L,j},t) \\ \langle\sin(n\varphi_L(t))\rangle_{\varphi_L} = 0 \end{cases}. \tag{42}$$

Now, the dynamics is evaluated by averaging the three-qubit density matrix $\rho(\{\gamma_j\}, t)$ for specific values of the switching rates γ in a range $[\gamma_1, \gamma_2]$ as follows:

$$\rho_{\rm de}(t) = \int_{\gamma_1}^{\gamma_2}\int_{\gamma_1}^{\gamma_2}\int_{\gamma_1}^{\gamma_2} \rho_{\rm de}(\{\gamma_j\}, t) P_\alpha(\{\gamma_{a,j}\}) P_\alpha(\{\gamma_{b,j}\}) P_\alpha(\{\gamma_{c,j}\})\, {\rm d}\{\gamma_{a,j}\}\, {\rm d}\{\gamma_{b,j}\}\, {\rm d}\{\gamma_{c,j}\}, \tag{43}$$

$$\rho_{\rm mix}(t) = \int_{\gamma_1}^{\gamma_2}\int_{\gamma_1}^{\gamma_2} \rho_{\rm mix}(\gamma_{a,j}, \gamma_{c,j}, t) P_\alpha(\{\gamma_{a,j}\}) P_\alpha(\{\gamma_{c,j}\})\, {\rm d}\{\gamma_{a,j}\}\, {\rm d}\{\gamma_{c,j}\}, \tag{44}$$

and

$$\rho_{\rm ce}(t) = \int_{\gamma_1}^{\gamma_2} \rho_{\rm ce}(\gamma_j, t) P_\alpha(\{\gamma_j\})\, {\rm d}\{\gamma_j\}, \tag{45}$$

with $P_\alpha(\{\gamma_{L,j}\}) \equiv \prod_{j=1}^{N} P_\alpha(\gamma_{L,j})$ and $d\{\gamma_{L,j}\} \equiv \prod_{j=1}^{N} d\gamma_{L,j}$. Once the average over γ is performed, the time-evolved density matrix $\rho_{\rm de}(t)$, $\rho_{\rm mix}(t)$ and $\rho_{\rm ce}(t)$ also in this configuration can be expressed in terms of time-dependent coefficient $\Gamma_{\rm de}(t)$ and $\Gamma_{\rm ce}(t)$ with

$$\Gamma_{\rm de,ce}(t) = [H_{\rm de,ce}(t)]^N, \tag{46}$$

where $H_{\rm de,ce}(t)$ are given in eq. (36).

4 Results

In this section, we present the analytical expressions and the time evolution of tripartite negativity, entanglement witness and decoherence in the physical model introduced in the previous section. The dynamics of quantum correlations is investigated for the GHZ state in the cases of different, mixed and common system-environment interaction as depicted in fig. 1. It is important to note that the analytical expressions for quantum discord are not presented because unlike other measures, we need to use numerical techniques to optimize the conditional entropies appearing in its definition.

4.1 Static noise

4.1.1 Different environments

Performing the calculation starting from the definitions given in eqs. (1), (2) and (4), the tripartite negativity $\mathcal{N}^{(3)}$, the expectation value of $\mathcal{W}_{\rm GHZ1}$ and the time evolution of decoherence $\varepsilon_\vartheta(t)$ can be expressed in term of time-dependent coefficient $\xi_{\rm de}(t)$ as

$$\mathcal{N}^{(3)} = \xi_{\rm de} + \frac{1}{2}\left(|1+\xi_{\rm de}| + |1-\xi_{\rm de}|\right) - 1, \tag{47}$$

$${\rm Tr}\left[\mathcal{W}_{\rm GHZ1}\rho_{\rm de}(t)\right] = \frac{1}{4}\left[1 - 3\xi_{\rm de}\cos^2(2\lambda t \Delta_0)\right], \tag{48}$$

and

$$\varepsilon_\vartheta(t) = -\frac{3}{4}(1-\xi_{\rm de})\ln\frac{1}{4}(1-\xi_{\rm de}) - \frac{1}{4}(1+3\xi_{\rm de})\ln\frac{1}{4}(1+3\xi_{\rm de}), \tag{49}$$

where $\xi_{\rm de} = \left[\frac{\sin(\lambda t \Delta_m)}{\lambda t \Delta_m}\right]^2$. It is important to note that such a result clearly shows a non-monotonic time decay of quantum correlations as expected from the non-Markovian nature of the static noise. In fig. 2, we have plotted the time evolution of $\mathcal{N}^{(3)}$, the opposite of the expectation value of $\mathcal{W}_{\rm GHZ1}$, the decoherence $\varepsilon_\vartheta(t)$ and quantum discord for different values of Δ_m.

As shown in fig. 2, entanglement is a damped oscillating function of time, thus showing peculiar phenomena as sudden death and revivals whereas QD decays exponentially to zero and finally vanishes. Such behaviours are in good agreement with the results described in ref. [16]. Note that the presence of peculiar phenomena of entanglement sudden death (ESD) and sudden birth (ESB) indicating that there is a back-flow of information from the environment to the system and vice versa. As there is not interaction between three independent qubits, this revival phenomenon is due to single qubit non-Markovian dynamics, which takes memory effect of the environment into account [64]. Decoherence as shown in fig. 2 is a monotonic function of time, and reaches asymptotic value. As expected, when the disorder of the environment, here quantified by the parameter Δ_m, increases, quantum correlations, quantified in terms of tripartite negativity and quantum discord, decay faster. The same qualitative behaviour is shown by decoherence as displayed

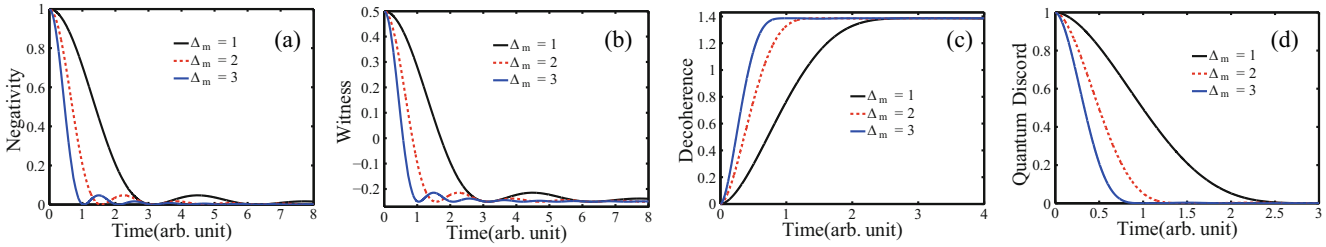

Fig. 2. Time evolution of tripartite negativity (a), opposite of the expectation value of $\mathcal{W}_{\mathrm{GHZ1}}$ (b), the decoherence (c) and quantum discord (d) for different values of Δ_m, when the three qubits are subjected to a static noise in different environments.

in the panel (c) of fig. 2, where the decoherence speed of the system increases as Δ_m increases. In fact, by increasing the parameter the revivals amplitude of $\mathcal{N}^{(3)}$ decreases and the oscillations tend to disappear while the saturation value of the decoherence remains constant. Furthermore, quantum entanglement quantified by the tripartite negativity result to be higher than the one detected by means of tripartite entanglement witness. On the other hand, the time behaviour exhibited by the entanglement witness shows that the witness operator given in eq. (2) is inefficient to detect the revivals of entanglement. Specially speaking, the residual amount of entanglement quantified by tripartite negativity is not detectable by means of the entanglement witness when the expectation value of $\mathcal{W}_{\mathrm{GHZ1}}$ becomes zero.

4.1.2 Mixed environments

In this configuration, the analytical expressions of the time-evolved tripartite negativity $\mathcal{N}^{(3)}$, the expectation value of $\mathcal{W}_{\mathrm{GHZ1}}$ and the time evolution of decoherence $\varepsilon_\vartheta(t)$ can be expressed as

$$\mathcal{N}^{(3)}(t) = \frac{1}{4}\left(|1+\xi_{\mathrm{ce}}+\eta| + |1+\xi_{\mathrm{ce}}-\eta|\right) + \frac{1}{2}\left(|1-\xi_{\mathrm{de}}| + |1+\xi_{\mathrm{de}}|\right) - 1, \tag{50}$$

$$\mathrm{Tr}\left[\mathcal{W}_{\mathrm{GHZ1}}\rho_{\mathrm{mix}}(t)\right] = -\frac{1}{8}\left(\xi_{\mathrm{ce}} + 4\xi_{\mathrm{de}} - 1\right) \tag{51}$$

and

$$\varepsilon_\vartheta(t) = -\frac{1}{4}\left(1-\xi_{\mathrm{ce}}\right)\ln\left(1-\xi_{\mathrm{ce}}\right) - \frac{1}{8}\left(3+\xi_{\mathrm{ce}}+\eta'\right)\ln\left(3+\xi_{\mathrm{ce}}+\eta'\right) \tag{52}$$

$$- \frac{1}{8}\left(3+\xi_{\mathrm{ce}}-\eta'\right)\ln\left(3+\xi_{\mathrm{ce}}-\eta'\right) + \frac{1}{4}\left(11+\xi_{\mathrm{de}}\right)\ln 2, \tag{53}$$

where $\xi_{\mathrm{ce}}(t) = \frac{\sin(2\lambda t\Delta_m)}{2\lambda t\Delta_m}$, $\eta(t) = \sqrt{\xi_{\mathrm{ce}}^2 + 4\xi_{\mathrm{de}}^2 - 2\xi_{\mathrm{ce}} + 1}$ and $\eta'(t) = \sqrt{\xi_{\mathrm{ce}}^2 + 16\xi_{\mathrm{de}}^2 - 2\xi_{\mathrm{ce}} + 1}$.

Such result clearly shows that the tripartite negativity expressed in terms of time-dependent coefficients $\xi_{\mathrm{de}}(t)$ and ξ_{ce} is not totally destroyed for a sufficiently long period of time. Indeed at the limit of a sufficiently long period of time, both $\xi_{\mathrm{de}}(t)$ and ξ_{ce} tend to zero. As a consequence, the tripartite negativity reaches its saturation value, which is $1/2$.

In fig. 3, the dynamics of $\mathcal{N}^{(3)}$, opposite of the expectation value of $\mathcal{W}_{\mathrm{GHZ1}}$, and quantum discord are shown for different values of Δ_m. We find that both $\mathcal{N}^{(3)}$ and the opposite of the expectation value of $\mathcal{W}_{\mathrm{GHZ1}}$ decay monotonically with time and exhibit damped oscillations after reaching their corresponding saturation values, whereas QD decays monotonically with time to zero and no sudden death and revivals phenomena are observed. Unlike the case of local system-environment interaction, here quantum entanglement can survive the decohering effects due to the static noise. Indeed, in agreement with ref. [16] when two of the qubits are coupled with a common environment, the latter can be interpreted as a sort of interaction mediator between the qubits themselves. Such an interaction somehow contributes to build up quantum correlations even if decohering effects of the environment are still dominant and lead to a power-like decaying profile of entanglement [16]. Also for this configuration we can see that quantum correlations, quantified in terms of tripartite negativity, $\mathcal{D}^{(3)}$ and $\mathcal{W}_{\mathrm{GHZ1}}$, decay faster when the disorder of environment is increased while the speed of decoherence of the system increases. It is important to note that the local minima of decoherence correspond to the local maxima of entanglement, thus suggesting a strict connection between the two quantities. On the other hand, quantum entanglement detected by the tripartite entanglement witness is lower than the one quantified by means of tripartite negativity. Furthermore, the behavior exhibited by the witness operator given in

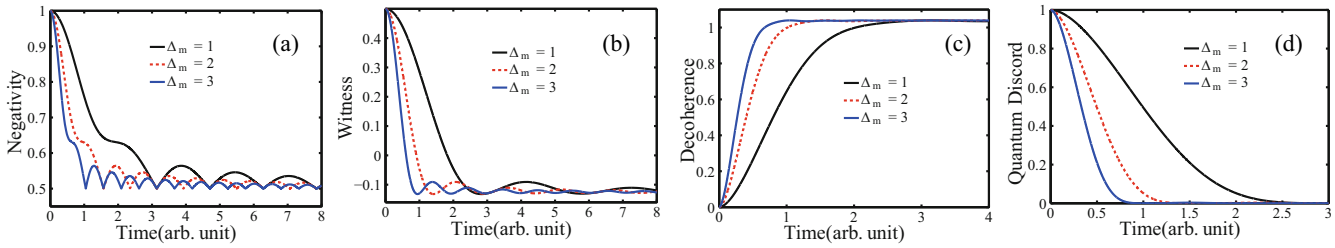

Fig. 3. Time evolution of tripartite negativity (a), opposite of the expectation value of $\mathcal{W}_{\mathrm{GHZ1}}$ (b), the decoherence (c) and quantum discord (d) for different values of Δ_m, when the qubits are subjected to a static noise in mixed environments.

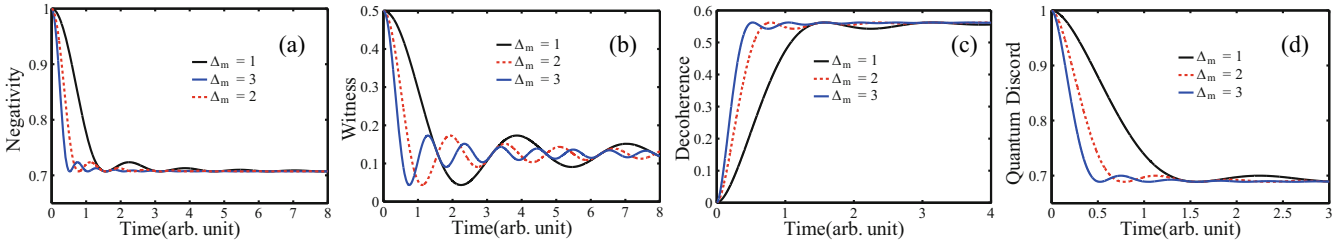

Fig. 4. Time evolution of tripartite negativity (a), opposite of the expectation value of $\mathcal{W}_{\mathrm{GHZ1}}$ (b), the decoherence (c) and quantum discord (d) for different values of Δ_m, when the qubits are coupled to a static noise in a common environment.

eq. (2) clearly demonstrates its inability to detect the long time preservation of entanglement as shown by tripartite negativity.

4.1.3 Common environment

Once more, the analytical expression of the time-evolved tripartite negativity $\mathcal{N}^{(3)}$, the expectation value of $\mathcal{W}_{\mathrm{GHZ1}}$ and the time evolution of decoherence $\varepsilon_\vartheta(t)$ can be expressed in terms of time-dependent coefficient ξ_{ce} as

$$\mathcal{N}^{(3)}(t) = \frac{1}{2}\sqrt{2\left(1+\xi_{\mathrm{de}}^2\right)} + \frac{1}{4}\left(|1+\xi_{\mathrm{ce}}| + |1-\xi_{\mathrm{ce}}|\right) - \frac{1}{2}, \tag{54}$$

$$\mathrm{Tr}\left[\mathcal{W}_{\mathrm{GHZ1}}\rho_{\mathrm{ce}}(t)\right] = -\frac{1}{8}\left[1+3\xi_{\mathrm{ce}}\cos(4\lambda t\Delta_0)\right] \tag{55}$$

and

$$\varepsilon_\vartheta(t) = -\left(\frac{1}{2}+\chi\right)\ln\left(\frac{1}{2}+\chi\right) - \left(\frac{1}{2}-\chi\right)\ln\left(\frac{1}{2}-\chi\right), \tag{56}$$

where $\chi = \frac{1}{4}\sqrt{(1+3\xi_{\mathrm{ce}}^2)}$. By analysing the analytical expressions obtained in this section one can immediately see that in the limit of a sufficiently long period of time, the entanglement is not completely destroyed. Indeed in the limit of the sufficiently long period of time, $\xi_{\mathrm{ce}}(t)$ goes to zero and $\mathcal{N}^{(3)}(t)$ reaches its saturation value while the expectation value of $\mathcal{W}_{\mathrm{GHZ1}}$ becomes negative. In fig. 4, the dynamics of $\mathcal{N}^{(3)}$, the opposite of the expectation value of $\mathcal{W}_{\mathrm{GHZ1}}$, the decoherence $\varepsilon_\vartheta(t)$ and quantum discord are shown for different values of Δ_m.

For this configuration, we find that both QD and tripartite negativity decay monotonically with time and exhibit damped oscillations after they reach their corresponding saturation values. Decoherence, unlike in the different- and mixed-environment interactions cases, presents evident oscillations before reaching the saturation value, thus suggesting an oscillatory decay of $\mathcal{N}^{(3)}$. The survival of $\mathcal{D}^{(3)}$ and tripartite negativity at a sufficiently long period of time represents the major discrepancy with what was found in the two-qubit model, analogously to the one here investigated [16]. Also in this configuration quantum correlation decays faster when Δ_m is increased. In agreement with previous findings [24], the partial preservation of the entanglement and QD can be, in this case, ascribed to the indirect interaction among the qubits stemming from the coupling of the global system to a common noisy environment. Unlike the different-environment interaction, here the environment no longer is only the source of decohering effects, but it also represents a sort of interaction mediator between the subsystems. Such an interaction somehow hinders the destruction of quantum correlations [24]. Finally, the time behavior exhibited by the opposite of $\langle\mathcal{W}_{\mathrm{GHZ1}}\rangle$, in this configuration, shows that the partial preservation of entanglement at a sufficiently long period of time can be successfully revealed by means of tripartite entanglement witness.

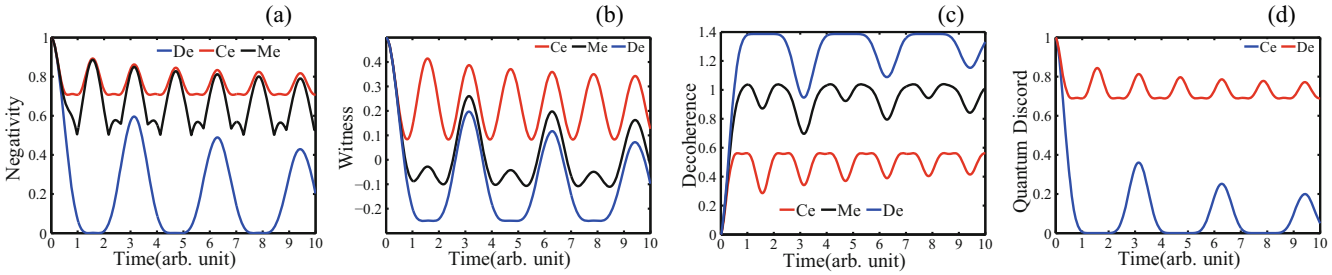

Fig. 5. Time evolution of negativity (a), opposite of the expectation values of $\mathcal{W}_{\mathrm{GHZ1}}$ (b), the decoherence (c) and QD (d) for three qubits interacting with a single random bistable fluctuator with $1/f$ spectrum in different (De), common (Ce) and mixed (Me) environments when $[\gamma_1, \gamma_2]/\lambda = [10^{-4}, 10^4]$.

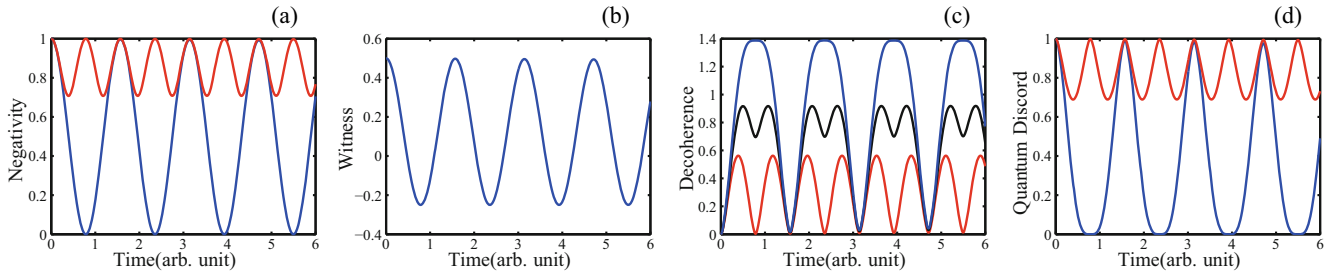

Fig. 6. Time evolution of negativity (a), opposite of the expectation values of EW (b), the decoherence (c) and QD (d) for three qubits interacting with a single random bistable fluctuator with $1/f^2$ spectrum in different (blue solid line), common (red solid line) and mixed (black solid line) environments when $[\gamma_1, \gamma_2]/\lambda = [10^{-4}, 10^4]$.

4.2 Colored noise

4.2.1 Single fluctuator

Here, the dynamics depends upon the selected range $[\gamma_1, \gamma_2]$ of the switching rate. Using again the definitions of eqs. (1), (2) and (4), we find that the tripartite negativity, the expectation value of $\mathcal{W}_{\mathrm{GHZ1}}$ and the decoherence $\varepsilon_\vartheta(t)$ for different-, mixed- and common-system-environment interaction, has the same analytical expressions as in the case of static noise (here after taking $\Delta_0 = 0$) but with different time-dependent coefficients. Indeed, we have

$$\xi_{\mathrm{de,ce}}(t) \longrightarrow H_{\mathrm{de,ce}}(t), \tag{57}$$

where the time-dependent coefficients $H_{\mathrm{ce}}(t)$ and $H_{\mathrm{de}}(t)$ are given in eq. (36).

The dynamics of $\mathcal{N}^{(3)}$, $\mathcal{D}^{(3)}$, $\varepsilon_\vartheta(t)$ and the opposite of the expectation value of $\mathcal{W}_{\mathrm{GHZ1}}$ for the cases of pink and brown noise are, respectively, shown in figs. 5 and 6. The range of integration is $[\gamma_1, \gamma_2]/\lambda = [10^{-4}, 10^4]$.

Note that the integrals $H_{\mathrm{ce}}(t)$ and $H_{\mathrm{de}}(t)$ appearing in the analytical expressions of quantum correlations have been computed numerically. We can clearly see from fig. 5 that quantum correlations can exhibit peculiar phenomena, such as sudden death, revivals and long-time survival. Indeed, we find that, when the qubits are coupled to the noise in different environments, both the entanglement quantifies in terms of tripartite negativity, as stated above, and QD decays monotonically to zero displaying revivals and sudden death phenomena with damped amplitude. On the other hand, when the qubits are coupled to the noise in a common environment or in mixed environments, we find that entanglement decays monotonically with time until it reaches its saturation value and exhibits damped oscillations. In other words, both entanglement and QD are not totally destroyed when the subsystems are coupled to a common source of noise whereas both are totally destroyed when the qubits are coupled to the noise in different environments. As there is no interaction between the three independent qubits, this revival phenomenon is due to single qubit non-Markovian dynamics, which takes memory effect of the environment into account [64]. Note that the long time preservation of both quantum discord and entanglement has already been observed in bipartite systems interacting with quantum environments [65,66] and tripartite systems interaction with classical RTN [24]. It is worth noting that the survival of quantum correlation in the long time limit represents the major discrepancy with the corresponding result described in the two-qubit model analogously to the one here investigated [17,50]. There, both bipartite entanglement and discord disappear at long times, regardless of the local or non-local character of the interaction among the qubits and the environment.

Furthermore, the entanglement and quantum discord quantify in terms of tripartite negativity and $\mathcal{D}^{(3)}$ is higher than the one detected by the tripartite entanglement witness. For all environmental situations, decoherence is a monotonic function of time, and presents damped oscillations after reaching the asymptotic value. These oscillations constitute a sufficient condition to signify the presence of memory effect of the environment.

Unlike the $1/f$ noise spectrum, here quantum correlations and decoherence are oscillating functions of time for all the analyzed configurations. We see that the entanglement exhibits the intriguing phenomena of entanglement sudden disappearance (ESD) and sudden birth (ESB), corresponding to an oscillating behavior of the decoherence curve (different environments). The periodicity of oscillations can be computed by analyzing the analytical expressions of the quantifiers of quantum correlations. In particular we can analyze the time-dependent coefficients, $\Phi_{2\lambda}$ and $\Phi_{4\lambda}$, appearing in the integral of eq. (36). Once more, quantum correlations are partially preserved when the qubits are coupled in a common environment. Furthermore, we note that, even if the analytical expressions of $\mathcal{N}_{\rm ce}^{(3)}$ and $\mathcal{D}_{\rm de}^{(3)}$ is different from those of $\mathcal{N}_{\rm mix}^{(3)}$ and $\mathcal{D}_{\rm mix}^{(3)}$, we find after numerical simulation that the curves of $\mathcal{N}_{\rm ce}^{(3)}$ and $\mathcal{D}_{\rm de}^{(3)}$ coincide with those of $\mathcal{N}_{\rm mix}^{(3)}$ and $\mathcal{D}_{\rm mix}^{(3)}$, respectively.

4.2.2 Collection of fluctuators

In the case of qubits interacting with a collection of fluctuators with fixed switching rates, the dynamics is very different, depending on the spectrum of the noise. Once again, following the definition of tripartite negativity given in eq. (1) and the one of entanglement witness and decoherence given in eqs. (2) and (4), we find that the tripartite negativity and the entanglement witness, for different-, mixed- and common-system-environment interaction, the same mathematical expressions as in the case of single fluctuator but with different time-dependent coefficients. Indeed, we have

$$H_{\rm ce,de}(t) \longrightarrow \Gamma_{\rm ce,de} = \left[H_{\rm ce,de}(t)\right]^N . \tag{58}$$

The dynamics of negativity, quantum discord, decoherence and EW for three qubits interacting with environments, consisting in a collection of N bistable fluctuators with $1/f$ spectrum are shown in fig. 7.

In agreement with previous investigations [47], we consider 20 sources of RTN as the minimum number of fluctuator needed to obtain both a reliable profile of the frequency spectrum and a representative sample of the $P(\gamma)$ distribution. In fig. 4, we report the behaviors of quantum correlations in the case of 20 and 150 fluctuators. Depending on the type of system-environment interaction, we find that all the quantifiers of quantum correlations decay exponentially with time either to a certain saturation value or to zero. Such a behaviors compared to the one displayed in fig. 5, clearly demonstrates that the mere knowledge of the spectrum is not sufficient to determine the dynamical evolution of quantum correlations. Indeed, we find that when the three-qubit system interacts with only one decoherence channel, intriguing phenomena of revival appear because the system is affected only by one source of classical noise and the information can flow back. As it can be clearly seen, when the number of decoherence channels is increased, the quantum correlation decays faster. We find that the same qualitative behavior is found for both entanglement and discord; this is due to the fact that the idea of quantum discord is to quantify all types of quantum correlations including entanglement. Thus, quantum discord is a function of entanglement. Note that it is also possible to obtain a pink noise spectrum even with a smaller number of fluctuators, but the problem is that this approximation does not describe a sample of $1/\gamma$-distributed switching rates. Unlike what was found in the two-qubit model, analogously to the one here investigated, both entanglement and QD are not totally destroyed when the qubits are coupled in a common environment. On the other hand, we find that quantum correlations are completely destroyed when the subsystems are coupled to the noise in different environments. The long-time preservation of quantum correlations can here be ascribed to the indirect interaction among the qubits. Furthermore, in the case of mixed environmental noise, we find that QD is totally destroyed while entanglement is preserved. The smaller is the number of fluctuator, the less degraded are the quantum correlations. Such a result allows us to conclude that entanglement in this work appears to be more robust against decoherence than QD.

The dynamics of negativity, discord and EW for three qubits interacting with environments, consisting in a collection of N bistable fluctuators with $1/f^2$ spectrum are shown in fig. 8. It can be clearly seen, from this figure, that a very different behavior arises when the qubits are coupled to environments, consisting in a collection of N bistable fluctuators with $1/f^2$ spectrum. Indeed, we find that quantum correlations decay exponentially with smooth damped oscillations. We find that, when the subsystems are coupled to a common source of noise, peculiar phenomena of sudden death and revivals appear for both entanglement and discord. We observe in all analyzed system-environment configurations that the heights of the oscillation peaks decrease when the number of fluctuators is increased. Once more, the long-time preservation of entanglement is found when the qubits are coupled either in a common environment or in mixed environments. Unlike $1/f$ spectrum, here we find that the witness, irrespective of the type of system-environment interaction, is able to detect the presence of tripartite entanglement at sufficiently long but finite time and that the ability of the tripartite entanglement witness to detect entanglement is weaker than that of tripartite negativity.

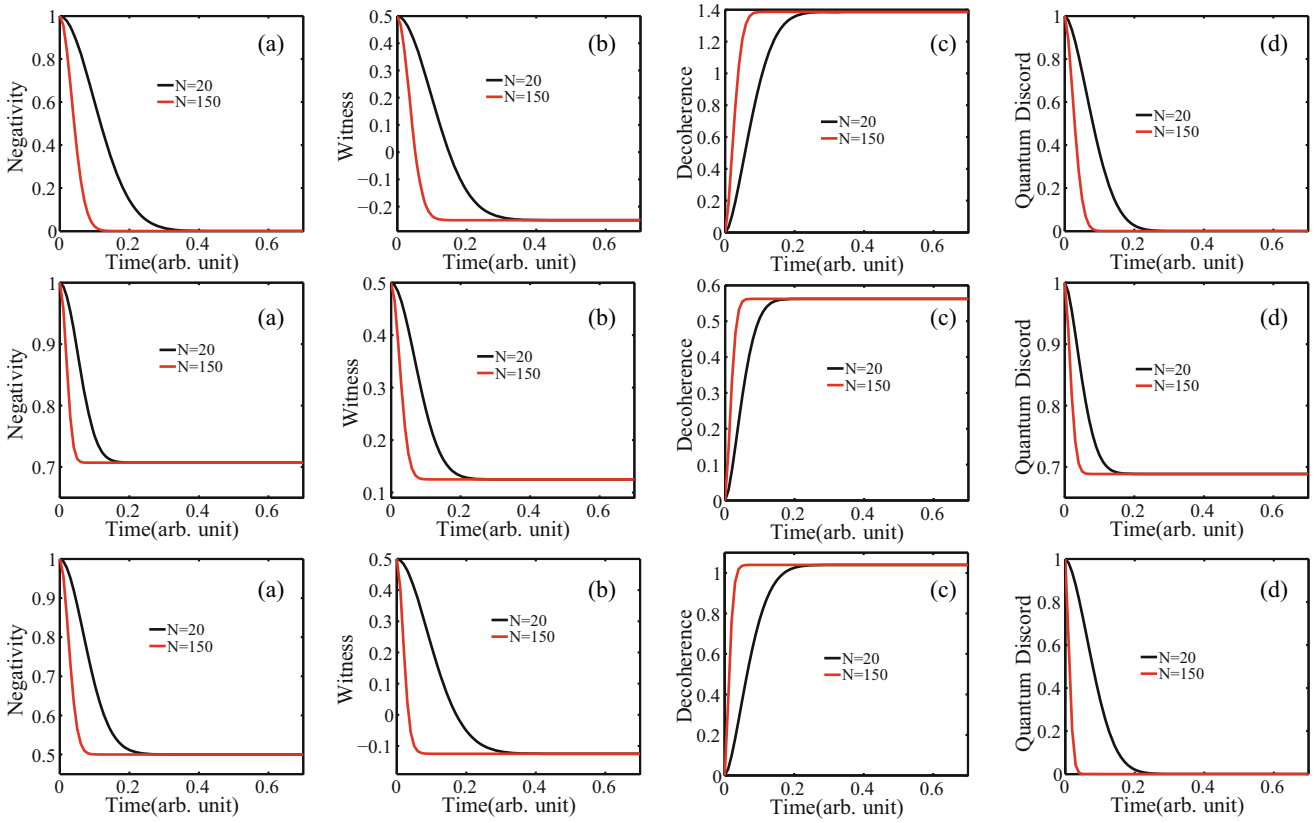

Fig. 7. Upper panels: Time evolution of tripartite negativity (a), opposite of the expectation value of $\mathcal{W}_{\mathrm{GHZ1}}$ (b), the decoherence (c) and quantum discord (d) for three qubits interacting in different environments, consisting in a collection of $N = 20$ (black solid line) and $N = 150$ (red solid line) bistable fluctuators with $1/f$ spectrum. Middle panels: the same but with qubits subject to a common environment. Lower panels: the same but with qubits subject to mixed environments.

5 Conclusions

In this paper we have analyzed in detail the decoherence and the dynamics of quantum correlations (entanglement and discord), for a system of three non-interacting qubits initially prepared in a maximally entangled GHZ state and then subjected to classical environmental noise modeled through a stochastic process. We computed the time-evolved density matrix of the three qubits by performing the ensemble average over the stochastic process, in the case of different, common and mixed environments. Negativity, decoherence, QD and entanglement witness have been computed, using both analytical and numerical techniques.

We showed that, starting from a maximally entangled GHZ state, the quantum correlations display different decaying behaviors, depending on the type of the system-environment interaction and the considered noise.

In particular, for static environmental noise, we found that the decay speed of quantum correlations and the speed of decoherence of the system are strongly affected by the disorder of the environment quantified by the parameter Δ_m. Indeed we showed that when the parameter Δ_m is increased, quantum correlations display a faster decay and the speed of decoherence of the system increases.

In the other kind of noise, that is colored noise, the dynamics of quantum correlations have been investigated for two different configurations of the environment. In the first configuration we have addressed, the three qubits interact with a single bistable fluctuator, which has a random switching rate leading to an overall $1/f^{\alpha}$ spectrum. In the second configuration, the three qubits interact with a collection of bistable fluctuators, each one with fixed switching rate, selected from a specific distribution $P_{\alpha}(\gamma)$. In the first configuration we found that quantum correlations display oscillation behavior with sudden death and revivals phenomena for both pink and brown noise. But in the case of pink noise, the oscillation amplitude of quantum correlations decays faster than in the case of brown noise. In the second configuration we found that the dynamics of quantum correlations depends upon the color of the noise and the number of fluctuators used to model the environment. Indeed, we find that quantum correlations show a monotonic decay when $\alpha = 1$ (pink noise), while peculiar phenomena of sudden death and revivals occur when $\alpha = 2$ (brown noise) and that the speed of disentanglement (loss of entanglement) and decoherence increases faster when the number of fluctuators used to model the environment is increasing.

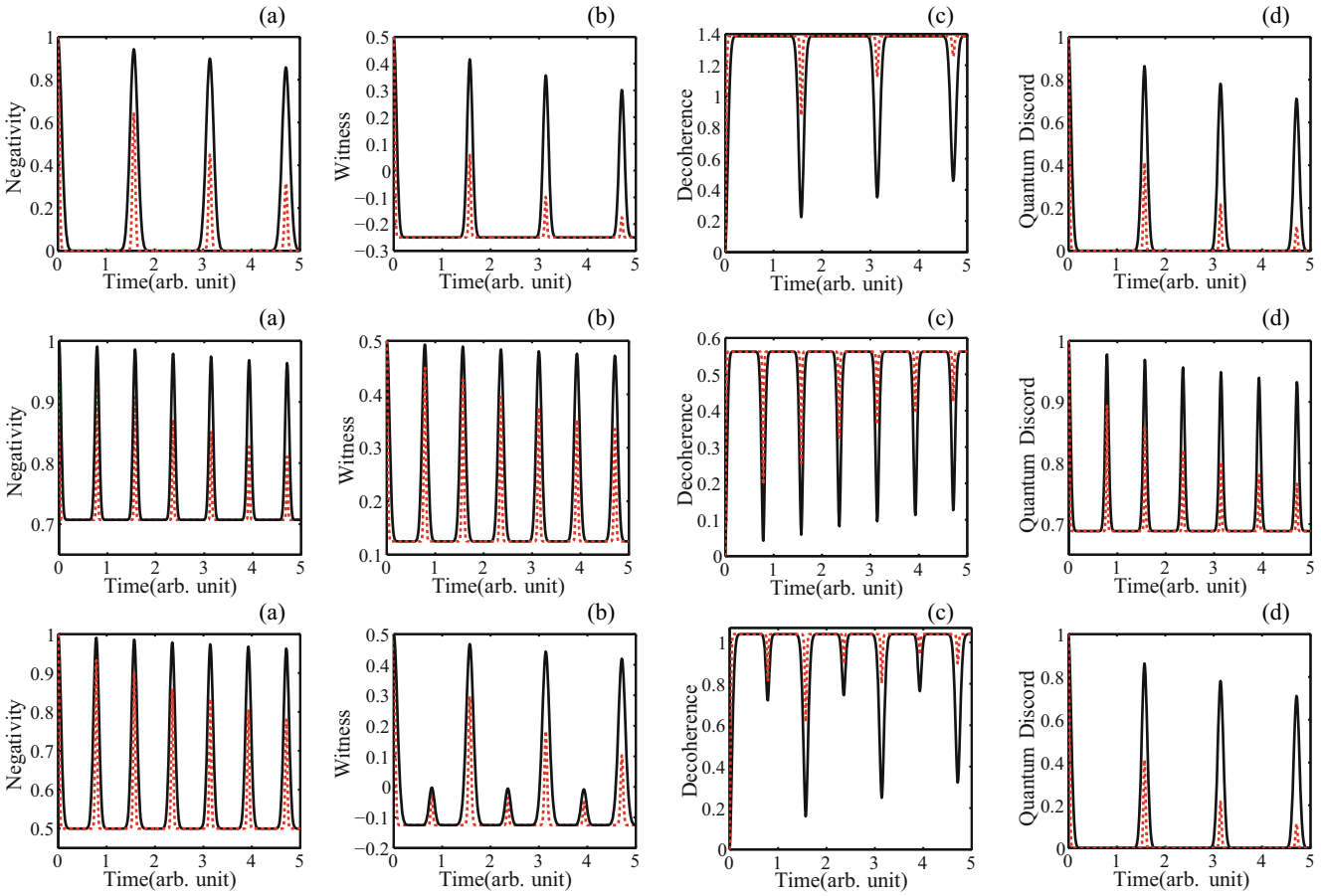

Fig. 8. Upper panels: Time evolution of tripartite negativity (a), opposite of the expectation value of $\mathcal{W}_{\mathrm{GHZ1}}$ (b), the decoherence (c) and quantum discord (d) for three qubits interacting in different environments, consisting in a collection of $N = 20$ (black solid line) and $N = 150$ (red dashed line) bistable fluctuators with $1/f^2$ spectrum. Middle panels: the same, but with qubits subject to a common environment. Lower panels: the same, but with qubits subject to mixed environments.

For both static and colored noises, our results highlight that quantum correlations can survive the decohering effects due to the noise when the qubits are coupled in a common environment, while they are completely destroyed when the qubits are coupled in different environments. We also found that both entanglement and QD display the same qualitative behavior demonstrating that there is a strict connection between the two quantities. On the other hand, our results clearly show that the action of different, common or mixed environments has different effects on the robustness of quantum correlations. Indeed we show that common environment followed by mixed environment degrade quantum correlations more weakly than different environments. Finally, we find that the survived entanglement can be efficiently detected by means of the entanglement witness when the qubits are affected by a common source of noise.

We believe that our analysis is helpful for a better understanding of the effects of classical environmental noise on the dynamics of quantum correlations in open tripartite quantum systems.

Appendix A. Evaluation of the time-evolved density matrix of the system: the case of static noise

Here, we give the explicit forms of the time-evolved density matrix, for different, mixed and common environments.

Appendix A.1. Different environments

We find that when the subsystems are coupled to the noise in different environments, the time-evolved density matrix

of the system, as defined in eq. (24), takes the following form:

$$\rho_{\rm de}(t) = \frac{1}{2}\begin{pmatrix} \rho_{11} & \rho_{12} & \rho_{12} & \rho_{12} & \rho_{12} & \rho_{12} & \rho_{12} & \rho_{11} \\ \rho_{21} & \rho_{22} & \rho_{23} & \rho_{23} & \rho_{23} & \rho_{23} & \rho_{22} & \rho_{21} \\ \rho_{21} & \rho_{23} & \rho_{22} & \rho_{23} & \rho_{23} & \rho_{22} & \rho_{23} & \rho_{21} \\ \rho_{21} & \rho_{23} & \rho_{23} & \rho_{22} & \rho_{22} & \rho_{23} & \rho_{23} & \rho_{21} \\ \rho_{21} & \rho_{23} & \rho_{23} & \rho_{22} & \rho_{22} & \rho_{23} & \rho_{23} & \rho_{21} \\ \rho_{21} & \rho_{23} & \rho_{22} & \rho_{23} & \rho_{23} & \rho_{22} & \rho_{23} & \rho_{21} \\ \rho_{21} & \rho_{22} & \rho_{23} & \rho_{23} & \rho_{23} & \rho_{23} & \rho_{22} & \rho_{21} \\ \rho_{11} & \rho_{12} & \rho_{12} & \rho_{12} & \rho_{12} & \rho_{12} & \rho_{12} & \rho_{11} \end{pmatrix}, \tag{A.1}$$

with

$$\rho_{11} = \frac{1}{4} + 3\left(\frac{\sin(\lambda t\Delta_m)\cos(2\lambda t\Delta_0)}{2\lambda t\Delta_m}\right)^2, \qquad \rho_{22} = \frac{1}{4} - \left(\frac{\sin(\lambda t\Delta_m)\cos(2\lambda t\Delta_0)}{2\lambda t\Delta_m}\right)^2,$$
$$\rho_{23} = \left(\frac{\sin(\lambda t\Delta_m)\sin(2\lambda t\Delta_0)}{2\lambda t\Delta_m}\right)^2,$$
$$\rho_{12} = -\left(\frac{\sin(\lambda t\Delta_m)}{2\lambda t\Delta_m}\right)^2 \left[i\sin(4\lambda t\Delta_0) + \sin(2\lambda t\Delta_0)^2\right] \quad \text{and} \quad \rho_{21} = -\left(\frac{\sin(\lambda t\Delta_m)}{2\lambda t\Delta_m}\right)^2 \left[i\sin(4\lambda t\Delta_0) - \sin(2\lambda t\Delta_0)^2\right].$$

Appendix A.2. Mixed environments

When all the three qubits are coupled to mixed source of static noise, the explicit evaluation of the time-evolved density matrix of the system takes the form

$$\rho_{\rm mix}(t) = \frac{1}{2}\begin{pmatrix} \rho_{11} & \rho_{12} & \rho_{13} & \rho_{13} & \rho_{13} & \rho_{13} & \rho_{12} & \rho_{11} \\ \rho_{21} & \rho_{22} & \rho_{24} & \rho_{24} & \rho_{24} & \rho_{24} & \rho_{22} & \rho_{21} \\ \rho_{31} & \rho_{32} & \rho_{33} & \rho_{33} & \rho_{33} & \rho_{33} & \rho_{32} & \rho_{31} \\ \rho_{31} & \rho_{32} & \rho_{33} & \rho_{33} & \rho_{33} & \rho_{33} & \rho_{32} & \rho_{31} \\ \rho_{31} & \rho_{32} & \rho_{33} & \rho_{33} & \rho_{33} & \rho_{33} & \rho_{32} & \rho_{31} \\ \rho_{31} & \rho_{32} & \rho_{33} & \rho_{33} & \rho_{33} & \rho_{33} & \rho_{32} & \rho_{31} \\ \rho_{21} & \rho_{22} & \rho_{24} & \rho_{24} & \rho_{24} & \rho_{24} & \rho_{22} & \rho_{21} \\ \rho_{11} & \rho_{12} & \rho_{13} & \rho_{13} & \rho_{13} & \rho_{13} & \rho_{12} & \rho_{11} \end{pmatrix}, \tag{A.2}$$

with

$$\rho_{11} = \frac{\sin(2\lambda t\Delta_m)\cos(4\lambda t\Delta_0)}{16(\lambda t\Delta_m)} + \frac{1}{2}\left(\frac{\cos(2\lambda t\Delta_0)\sin(\lambda t\Delta_m)}{\lambda t\Delta_m}\right)^2 + \frac{3}{8},$$
$$\rho_{12} = \frac{-i\sin^2(\lambda t\Delta_m)\sin(4\lambda t\Delta_0)}{(2\lambda t\Delta_m)^2} + \frac{\sin(2\lambda t\Delta_m)\cos(4\lambda t\Delta_0)}{16(\lambda t\Delta_m)} - \frac{1}{8},$$
$$\rho_{22} = \frac{\sin(2\lambda t\Delta_m)\cos(4\lambda t\Delta_0)}{16(\lambda t\Delta_m)} - \frac{1}{2}\left(\frac{\cos(2\lambda t\Delta_0)\sin(\lambda t\Delta_m)}{\lambda t\Delta_m}\right)^2 + \frac{3}{8}, \qquad \rho_{33} = -\frac{\sin(2\lambda t\Delta_m)\cos(4\lambda t\Delta_0)}{16(\lambda t\Delta_m)} + \frac{1}{8},$$
$$\rho_{21} = \frac{i\sin^2(\lambda t\Delta_m)\sin(4\lambda t\Delta_0)}{(2\lambda t\Delta_m)^2} + \frac{\sin(2\lambda t\Delta_m)\cos(4\lambda t\Delta_0)}{16(\lambda t\Delta_m)} - \frac{1}{8},$$
$$\rho_{13} = \frac{i}{4}\left[-\frac{\sin(2\lambda t\Delta_m)}{4(\lambda t\Delta_m)} - \frac{1}{2}\left(\frac{\sin(\lambda t\Delta_m)}{\lambda t\Delta_m}\right)^2\right]\sin(4\lambda t\Delta_0) - \left(\frac{\sin(\lambda t\Delta_m)\sin(2\lambda t\Delta_0)}{(2\lambda t\Delta_m)}\right)^2,$$
$$\rho_{24} = \frac{i}{4}\left[-\frac{\sin(2\lambda t\Delta_m)}{4(\lambda t\Delta_m)} + \frac{1}{2}\left(\frac{\sin(\lambda t\Delta_m)}{\lambda t\Delta_m}\right)^2\right]\sin(4\lambda t\Delta_0) + \left(\frac{\sin(\lambda t\Delta_m)\sin(2\lambda t\Delta_0)}{(2\lambda t\Delta_m)}\right)^2,$$

$$\rho_{31} = \frac{i}{4}\left[\frac{\sin(2\lambda t\Delta_m)}{4(\lambda t\Delta_m)} + \frac{1}{2}\left(\frac{\sin(\lambda t\Delta_m)}{\lambda t\Delta_m}\right)^2\right]\sin(4\lambda t\Delta_0) - \left(\frac{\sin(\lambda t\Delta_m)\sin(2\lambda t\Delta_0)}{(2\lambda t\Delta_m)}\right)^2,$$
$$\rho_{13} = \frac{i}{4}\left[\frac{\sin(2\lambda t\Delta_m)}{4(\lambda t\Delta_m)} - \frac{1}{2}\left(\frac{\sin(\lambda t\Delta_m)}{\lambda t\Delta_m}\right)^2\right]\sin(4\lambda t\Delta_0) + \left(\frac{\sin(\lambda t\Delta_m)\sin(2\lambda t\Delta_0)}{(2\lambda t\Delta_m)}\right)^2.$$

Appendix A.3. Common environment

On the other hand, when the subsystems are coupled with the same source of noise, *i.e.* in common environment, the time-evolved density matrix can be written as

$$\rho_{\mathrm{ce}}(t) = \frac{1}{16}\begin{pmatrix} \rho_{11} & \rho_{12} & \rho_{12} & \rho_{12} & \rho_{12} & \rho_{12} & \rho_{12} & \rho_{11} \\ \rho_{21} & \rho_{22} & \rho_{22} & \rho_{22} & \rho_{22} & \rho_{22} & \rho_{22} & \rho_{21} \\ \rho_{21} & \rho_{22} & \rho_{22} & \rho_{22} & \rho_{22} & \rho_{22} & \rho_{22} & \rho_{21} \\ \rho_{21} & \rho_{22} & \rho_{22} & \rho_{22} & \rho_{22} & \rho_{22} & \rho_{22} & \rho_{21} \\ \rho_{21} & \rho_{22} & \rho_{22} & \rho_{22} & \rho_{22} & \rho_{22} & \rho_{22} & \rho_{21} \\ \rho_{21} & \rho_{22} & \rho_{22} & \rho_{22} & \rho_{22} & \rho_{22} & \rho_{22} & \rho_{21} \\ \rho_{21} & \rho_{22} & \rho_{22} & \rho_{22} & \rho_{22} & \rho_{22} & \rho_{22} & \rho_{21} \\ \rho_{11} & \rho_{12} & \rho_{12} & \rho_{12} & \rho_{12} & \rho_{12} & \rho_{12} & \rho_{11} \end{pmatrix}, \tag{A.3}$$

with

$$\rho_{11} = 5 + \frac{3\sin(2\lambda t\Delta_m)\cos(4\lambda t\Delta_0)}{2\lambda t\Delta_m}, \qquad \rho_{22} = 1 - \frac{\sin(2\lambda t\Delta_m)\cos(4\lambda t\Delta_0)}{2\lambda t\Delta_m},$$
$$\rho_{12} = \frac{\sin(2\lambda t\Delta_m)}{\lambda t\Delta_m}\left[\frac{1}{2}\cos(4\lambda t\Delta_0) - i\sin(4\lambda t\Delta_0)\right] - 1,$$
$$\text{and} \quad \rho_{21} = \frac{\sin(2\lambda t\Delta_m)}{\lambda t\Delta_m}\left[\frac{1}{2}\cos(4\lambda t\Delta_0) + i\sin(4\lambda t\Delta_0)\right] - 1.$$

Appendix B. Evaluation of the time-evolved density matrix of the system: the case of colored noise

Here, we give the explicit forms of the time-evolved density matrix, for different, mixed and common environments.

In order to evaluate the dynamics of the system, firstly, we calculate the evolution of the initial state for a given choice of noise parameter, the obtained density matrix is averaged over all the possible realizations of the noise phase and finally the resulting density matrix is averaged over the possible choices for the switching rates.

Appendix B.1. Different environments

We find that, in the case of local system-environment coupling, the time-evolved density matrix of the system takes the form

$$\rho_{\mathrm{de}}(t) = \frac{1}{8}\begin{pmatrix} \bar\rho_{11} & 0 & 0 & 0 & 0 & 0 & 0 & \bar\rho_{11} \\ 0 & \bar\rho_{22} & 0 & 0 & 0 & 0 & \bar\rho_{22} & 0 \\ 0 & 0 & \bar\rho_{22} & 0 & 0 & \bar\rho_{22} & 0 & 0 \\ 0 & 0 & 0 & \bar\rho_{22} & \bar\rho_{22} & 0 & 0 & 0 \\ 0 & 0 & 0 & \bar\rho_{22} & \bar\rho_{22} & 0 & 0 & 0 \\ 0 & 0 & \bar\rho_{22} & 0 & 0 & \bar\rho_{22} & 0 & 0 \\ 0 & \bar\rho_{22} & 0 & 0 & 0 & 0 & \bar\rho_{22} & 0 \\ \bar\rho_{11} & 0 & 0 & 0 & 0 & 0 & 0 & \bar\rho_{11} \end{pmatrix}, \tag{B.1}$$

where $\langle\rho_{11}\rangle = 1 + 3H_{\mathrm{de}}(t)$ and $\langle\rho_{22}\rangle = 1 - H_{\mathrm{de}}(t)$.

Appendix B.2. Mixed environments

When the three qubits are coupled to mixed sources of noise, the time-evolved density matrix of the system can be written as

$$\rho_{\mathrm{mix}}(t) = \frac{1}{2}\begin{pmatrix} \bar{\rho}_{11} & -\bar{\rho}_{33} & 0 & 0 & 0 & 0 & -\bar{\rho}_{33} & \bar{\rho}_{11} \\ -\bar{\rho}_{33} & \bar{\rho}_{22} & 0 & 0 & 0 & 0 & \bar{\rho}_{22} & -\bar{\rho}_{33} \\ 0 & 0 & \bar{\rho}_{33} & \bar{\rho}_{33} & \bar{\rho}_{33} & \bar{\rho}_{33} & 0 & 0 \\ 0 & 0 & \bar{\rho}_{33} & \bar{\rho}_{33} & \bar{\rho}_{33} & \bar{\rho}_{33} & 0 & 0 \\ 0 & 0 & \bar{\rho}_{33} & \bar{\rho}_{33} & \bar{\rho}_{33} & \bar{\rho}_{33} & 0 & 0 \\ 0 & 0 & \bar{\rho}_{33} & \bar{\rho}_{33} & \bar{\rho}_{33} & \bar{\rho}_{33} & 0 & 0 \\ -\bar{\rho}_{33} & \bar{\rho}_{22} & 0 & 0 & 0 & 0 & \bar{\rho}_{22} & -\bar{\rho}_{33} \\ \bar{\rho}_{11} & -\bar{\rho}_{33} & 0 & 0 & 0 & 0 & -\bar{\rho}_{33} & \bar{\rho}_{11} \end{pmatrix}, \tag{B.2}$$

with $\langle\rho_{11}\rangle = \frac{H_{\mathrm{ce}}}{8} + \frac{H_{\mathrm{de}}}{2} + \frac{3}{8}$, $\langle\rho_{22}\rangle = \frac{H_{\mathrm{ce}}}{8} - \frac{H_{\mathrm{de}}}{2} + \frac{3}{8}$ and $\langle\rho_{33}\rangle = -\frac{H_{\mathrm{ce}}}{8} + \frac{1}{8}$.

Appendix B.3. Common environment

On the other hand, for the case of non-local qubit-environment interaction, the time-evolved density matrix of the system results in

$$\rho_{\mathrm{ce}}(t) = \frac{1}{16}\begin{pmatrix} \bar{\rho}_{11} & -\bar{\rho}_{22} & -\bar{\rho}_{22} & -\bar{\rho}_{22} & -\bar{\rho}_{22} & -\bar{\rho}_{22} & -\bar{\rho}_{22} & \bar{\rho}_{11} \\ -\bar{\rho}_{22} & \bar{\rho}_{22} & \bar{\rho}_{22} & \bar{\rho}_{22} & \bar{\rho}_{22} & \bar{\rho}_{22} & \bar{\rho}_{22} & -\bar{\rho}_{22} \\ -\bar{\rho}_{22} & \bar{\rho}_{22} & \bar{\rho}_{22} & \bar{\rho}_{22} & \bar{\rho}_{22} & \bar{\rho}_{22} & \bar{\rho}_{22} & -\bar{\rho}_{22} \\ -\bar{\rho}_{22} & \bar{\rho}_{22} & \bar{\rho}_{22} & \bar{\rho}_{22} & \bar{\rho}_{22} & \bar{\rho}_{22} & \bar{\rho}_{22} & -\bar{\rho}_{22} \\ -\bar{\rho}_{22} & \bar{\rho}_{22} & \bar{\rho}_{22} & \bar{\rho}_{22} & \bar{\rho}_{22} & \bar{\rho}_{22} & \bar{\rho}_{22} & -\bar{\rho}_{22} \\ -\bar{\rho}_{22} & \bar{\rho}_{22} & \bar{\rho}_{22} & \bar{\rho}_{22} & \bar{\rho}_{22} & \bar{\rho}_{22} & \bar{\rho}_{22} & -\bar{\rho}_{22} \\ -\bar{\rho}_{22} & \bar{\rho}_{22} & \bar{\rho}_{22} & \bar{\rho}_{22} & \bar{\rho}_{22} & \bar{\rho}_{22} & \bar{\rho}_{22} & -\bar{\rho}_{22} \\ \bar{\rho}_{11} & -\bar{\rho}_{22} & -\bar{\rho}_{22} & -\bar{\rho}_{22} & -\bar{\rho}_{22} & -\bar{\rho}_{22} & -\bar{\rho}_{22} & \bar{\rho}_{11} \end{pmatrix}, \tag{B.3}$$

with $\langle\rho_{11}\rangle = 5 + 3H_{\mathrm{de}}$ and $\langle\rho_{22}\rangle = 1 - H_{\mathrm{de}}$.

References

1. M. Ramzan, Eur. Phys. J. D **67**, 170 (2013).
2. M.A. Nielsen, I.L. Chuang, *Quantum Computation and Quantum Information* (Cambridge University Press, 2010).
3. J.I. Cirac, P. Zoller, Phys. Rev. Lett. **74**, 4091 (1995).
4. C.H. Bennett, D.P. DiVincenzo, Nature **404**, 247 (2000).
5. C. Xie, Y. Liu, H. Xing *et al.*, Quantum Inf. Process. **14**, 653 (2015).
6. N. Gisin, G. Ribordy, W. Tittel, H. Zbinden, Rev. Mod. Phys. **74**, 145 (2002).
7. X. Li, Q. Pan, J. Jing, J. Zhang, C. Xie, K. Peng, Phys. Rev. Lett. **88**, 04790416 (2002).
8. Th. Richter, W. Vogel, Phys. Rev. A **76**, 053835 (2012).
9. M. Murao, D. Jonathan, M.B. Plenio, V. Vedral, Phys. Rev. A **59**, 156 (1999).
10. C.Y. Hu, J.G. Rarity, Phys. Rev. B **83**, 115303 (2011).
11. T. Yu, J.H. Eberly, Science **323**, 598 (2009).
12. L. Aolita, F. de Melo, L. Davidovich, Rep. Prog. Phys. **78**, 042001 (2015).
13. R. Lo Franco, Quantum Inf. Process. **15**, 2393 (2016).
14. T. Yu, J.H. Eberly, Phys. Rev. Lett. **93**, 140404 (2004).
15. N. Metwally, A.S. Obada, arXiv:1506.01036 (2015).
16. C. Benedetti, F. Buscemi, P. Bordone, M.G.A. Paris, Int. J. Quant. Inf. **10**, 1241005 (2012).
17. C. Benedetti, M.G.A. Paris, F. Buscemi, P. Bordone, *Time-evolution of entanglement and quantum discord of bipartite systems subject to* $1/f^{\alpha}$ *noise*, in *Proceedings of the 22nd International Conference on Noise and Fluctuations (ICNF) 2013 Montpellier* (IEEE, 2013) DOI: 10.1109/ICNF.2013.6578952.
18. D. Zhou, A. Lang, R. Joynt, Quantum Inf. Process. **9**, 727 (2010).
19. A. De, A. Lang, D. Zhou, R. Joynt, Phys. Rev. A **83**, 042331 (2011).
20. B. Leggio, R. Lo Franco, D.O. Soares-Pinto, P. Horodecki, G. Compagno, Phys. Rev. A **92**, 032311 (2015).

21. A. D'Arrigo, G. Benenti, R. Lo Franco, G. Falci, E. Paladino, Int. J. Quant. Inf. **12**, 1461005 (2014).
22. J.-S. Xu, K. Sun, C.-F. Li *et al.*, Nat. Commun. **4**, 2851 (2013).
23. A. Orieux, A. D'Arrigo, G. Ferranti, R.L. Franco *et al.*, Sci. Rep. **5**, 8575 (2015).
24. F. Buscemi, P. Bordone, Phys. Rev. A **87**, 042310 (2013).
25. W.K. Wootters, Phys. Rev. Lett. **80**, 2245 (1998).
26. M.C. Tichy, F. Mintert, A. Buchleitner, J. Phys. B: At. Mol. Opt. Phys. **44**, 192001 (2011).
27. R. Horodecki, P. Horodecki, M. Horodecki, K. Horodecki, Rev. Mod. Phys. **81**, 865 (2009).
28. L. Gurvits, in *Proceedings of the 35th Annual ACM Symposium on Theory of Computing* (AMC, New York, 2003) pp. 10–19.
29. L. Amico, R. Fazio, A. Osterloh, V. Vedral, Rev. Mod. Phys. **80**, 517 (2008).
30. Z.H. Chen, Z.H. Ma, J.L. Chen, S. Severini, Phys. Rev. A **85**, 062320 (2012).
31. Y.S. Weinstein, Phys. Rev. A **79**, 012318 (2009).
32. A. Acin, A. Andrianov, L. Costa, E. Jan, J.I. Latorre, R. Tarrach, Phys. Rev. Lett. **85**, 1560 (2000).
33. C.H. Bennett, D.P. DiVincenzo, C.A. Fuchs *et al.*, Phys. Rev. A **59**, 1070 (1999).
34. M. Horodecki, P. Horodecki, R. Horodecki, J. Oppenheim, A. Sen, U. Sen, B. Synak-Radtke, Phys. Rev. A **71**, 062307 (2005).
35. J. Niset, N.J. Cerf, Phys. Rev. A **74**, 052103 (2006).
36. J. Cui, H. Fan, J. Phys. A **43**, 045305 (2010).
37. B.P. Lanyon, M. Barbieri, M.P. Almeida, A.G. White, Phys. Rev. Lett. **101**, 200501 (2008).
38. Z. Jian-Song, C. Ai-Xi, Quant. Phys. Lett. **69**, 1 (2012).
39. K. Modi, A. Brodutch, H. Cable, T. Paterek, V. Vedral, Rev. Mod. Phys. **84**, 1655 (2012).
40. S. Luo, Phys. Rev. A **77**, 022301 (2008).
41. J. Maziero, L.C. C'eleri, R.M. Serra, V. Vedral, Phys. Rev. A **80**, 044102 (2009).
42. T. Werlang, S. Souza, F.F. Fanchini, C.J. Villas Boas, Phys. Rev. A **80**, 024103 (2009).
43. L. Mazzola, J. Piilo, S. Maniscalco, Phys. Rev. Lett. **104**, 200401 (2010).
44. J.-S. Xu, X.-Ye. Xu, C.-F. Li *et al.*, Nat. Commun. **1**, 7 (2010).
45. M. Cianciaruso, T.R. Bromley, W. Roga, R. Lo Franco, G. Adesso, Sci. Rep. **5**, 10177 (2015).
46. B. Aaronson, R. Lo Franco, G. Adesso, Phys. Rev. A **88**, 012120 (2013).
47. M.B. Weissman, Rev. Mod. Phys. **60**, 537 (1988).
48. G. Falci, A. D'arrigo, A. Mastellone, E. Paladino, Phys. Rev. Lett. **94**, 167002 (2005).
49. B. Bellomo, G. Compagno, A. D'Arrigo, G. Falci, R. Lo Franco, E. Paladino, Phys. Rev. A **81**, 062309 (2010).
50. C. Benedetti, F. Buscemi, P. Bordone, M.G.A. Paris, Phys. Rev. A **87**, 052328 (2013).
51. G.L. Giorgi, B. Bellomo, F. Galve, R. Zambrini, Phys. Rev. Lett. **107**, 190501 (2011).
52. C. Sabin, G. Garcia-Alcaine, Eur. Phys. J. D **48**, 435 (2008).
53. G.N. Matthew, PhD Thesis, University of California, Santa Barbara (2010).
54. A. Acin, D. Bruss, M. Lewenstein, A. Sanpera, Phys. Rev. Lett. **87**, 040401 (2001).
55. S. Bose, V. Vedral, Phys. Rev. A **61**, 040101 (2000).
56. A. Peres, *Quantum Theory: Concepts and Methods* (Kluwer Academic Publishers, Dordrecht, 1998).
57. C.H. Bennett, A. Grudka, M. Horodecki, P. Horodecki, R. Horodecki, Phys. Rev. A **83**, 012312 (2011).
58. L. Zhao, X. Hu, R. Yue *et al.*, Quantum Inf. Process. **12**, 2371 (2013).
59. A. Beggi, F. Buscemi, P. Bordone, Quantum Inf. Process. **14**, 573 (2015).
60. P. Bordone, F. Buscemi, C. Benedetti, Fluctuat. Noise Lett. **11**, 1242003 (2012).
61. E. Paladino, A. DArrigo, A. Mastellone, G. Falci, New J. Phys. **13**, 093037 (2011).
62. J. Bergli, Y.M. Galperin, B.L. Altshuler, New J. Phys. **11**, 025002 (2009).
63. B. Abel, F. Marquardt, Phys. Rev. B **78**, 201302 (2008).
64. Z. Zhu-Qiang, W. An-Min, Q. Liang, Commun. Theor. Phys. **50**, 1123 (2008).
65. J. Ma, Z. Sun, X. Wang, F. Nori, Phys. Rev. A **85**, 062323 (2012).
66. Z.-X. Man, Y.-J. Xia, R. Lo Franco, Sci. Rep. **5**, 13843 (2015).